

## Supporting information

### **High efficiency hysteresis-less inverted planar heterojunction perovskite solar cell with $\text{NiO}_x$ hole contact layer**

*Xingtian Yin\*, Meidan Que, Yonglei Xing, Wenxiu Que\**

**Electronic Materials Research Laboratory, International Center for Dielectric Research,**

**Key Laboratory of the Ministry of Education, School of Electronic & Information**

**Engineering, Xi'an Jiaotong University, Xi'an 710049, Shaanxi, People's Republic of China**

---

\* Corresponding author:

Email address: [xt\\_yin@mail.xjtu.edu.cn](mailto:xt_yin@mail.xjtu.edu.cn); [wxque@mail.xjtu.edu.cn](mailto:wxque@mail.xjtu.edu.cn)

Tel.: +86-29-83395679; Fax: +86-29-83395679

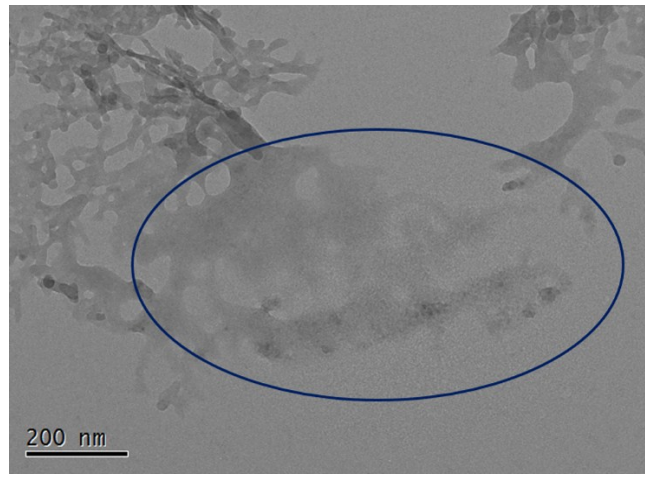


Figure S1: TEM image of the  $\text{NiO}_x$  nanoparticle precursor. The area indicated by the blue circle is irradiated by electron beams during TEM characterization. Obviously, the organic components which coat the  $\text{NiO}_x$  nanoparticles are destroyed by the electron beams.

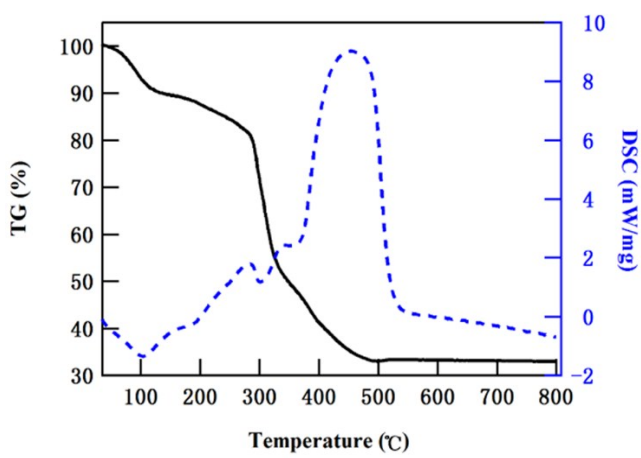


Figure S2 TGA and DSC curves of the  $\text{NiO}_x$  powder obtained by drying the precursor at  $150^\circ\text{C}$  for 20 min.

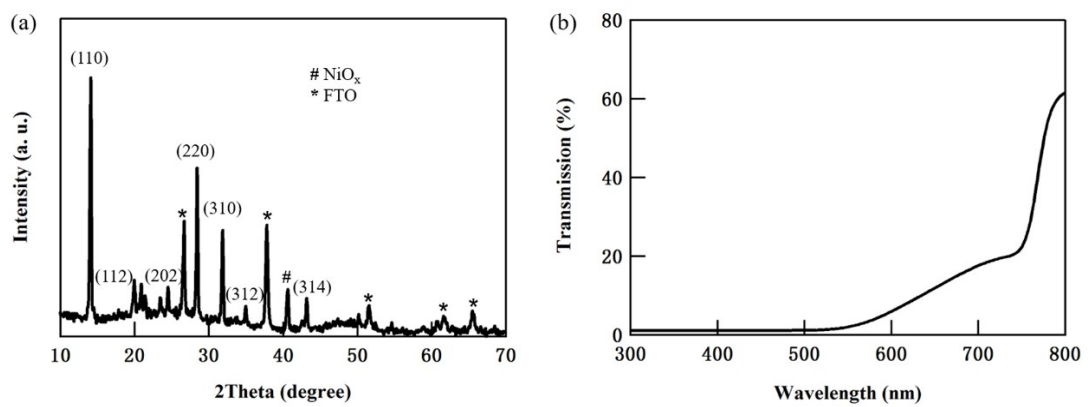


Figure S3 (a) XRD pattern (b) UV-Vis transmission spectrum of the perovskite film on the NiO<sub>x</sub> coated FTO substrate.

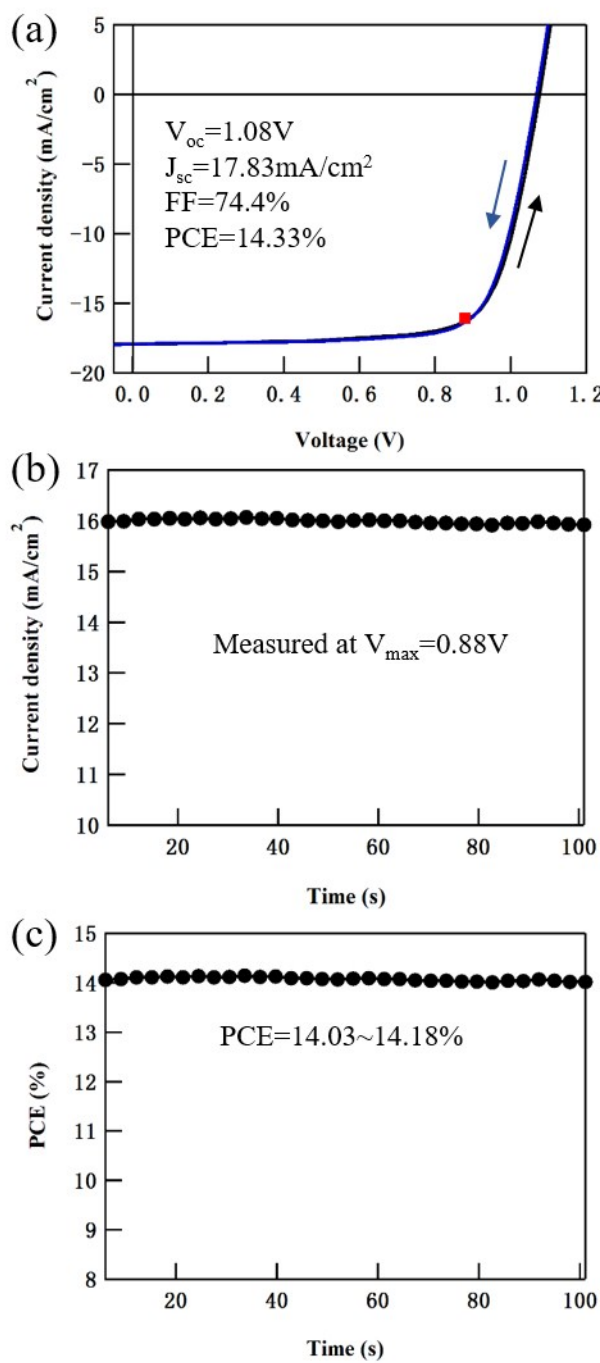


Figure S4. (a) J-V curves a device with 90 nm  $\text{NiO}_x$  film. The scan directions are indicated by the arrows and the red spot represents the maximum power point obtained from the steady state power conversion efficiency measurement. (b) The current density measured at 0.88V, which is the

voltage for the maximum power point shown in a. Clearly, the current density is stable as the time increases. (c) The steady state power conversion efficiency of the device.

Table S1 Summary on the performances of the reported  $\text{NiO}_x$ -based organic-inorganic hybrid perovskite solar cells and our devices are also included for comparison. The word “non” means the parameter was not presented in the paper.

Device configuration	$V_{oc}$ (V)	$J_{sc}$ (mA/cm <sup>2</sup> )	FF (%)	PCE (%)	Area (cm <sup>2</sup> )	Hysteresis ( PCE <sub>r</sub> -PCE <sub>f</sub>  ) %	Reference
ITO/PLD-NiO/CH <sub>3</sub> NH <sub>3</sub> PbI <sub>3</sub> /PCBM/LiF/Al	1.06	20.2	0.813	17.3	Non	Non	<sup>1</sup>
FTO/Cu:NiO/CH <sub>3</sub> NH <sub>3</sub> PbI <sub>3</sub> /PCBM/Ag	1.11±0.01	18.75±0.42	0.72±0.01	15.40±0.3 3	Non	obvious	<sup>2</sup>
FTO/TiO <sub>2</sub> /ZrO <sub>2</sub> /NiO/carbon-(CH <sub>3</sub> NH <sub>3</sub> PbI <sub>3</sub> )	0.917	21.36	0.76	14.9	Non	Non	<sup>3</sup>
<b>FTO/NiO<sub>x</sub>/CH<sub>3</sub>NH<sub>3</sub>PbI<sub>3</sub>/PCBM/Ag</b>	<b>1.09</b>	<b>17.93</b>	<b>73.8</b>	<b>14.42</b>	<b>0.07</b>	<b>0.06</b>	<b>This work</b>
FTO/NiO/Meso-Al <sub>2</sub> O <sub>3</sub> /CH <sub>3</sub> NH <sub>3</sub> PbI <sub>3</sub> /PCBM/BCP/Ag	1.04	18.0	72	13.5	0.09	0.66	<sup>4</sup>
ITO/ NiO/meso-NiO/CH <sub>3</sub> NH <sub>3</sub> PbI <sub>3</sub> /BCP/Al	0.96	19.8	61	11.6	Non	Non	<sup>5</sup>
FTO/ NiO NCs/CH <sub>3</sub> NH <sub>3</sub> PbCl <sub>3-x</sub> I <sub>x</sub> /PCBM (1.5 wt% PS)/Al	1.07	15.62	0.64	10.68	Non	Obvious	<sup>6</sup>
FTO/NiO/CH <sub>3</sub> NH <sub>3</sub> PbI <sub>3</sub> /PCBM/Ag	1.10	15.17	0.59	9.84	Non	Non	<sup>7</sup>
FTO/NiO NCs/CH <sub>3</sub> NH <sub>3</sub> PbI <sub>3</sub> /PCBM/Au	0.882	16.27	63.5	9.11	Non	Non	<sup>8</sup>
ITO/NiO/meso-NiO/CH <sub>3</sub> NH <sub>3</sub> PbI <sub>3</sub> /BCP/Al	1.04	13.24	69	9.51	0.06	Non	<sup>9</sup>
ITO/NiO/CH <sub>3</sub> NH <sub>3</sub> PbI <sub>3-x</sub> Cl <sub>x</sub> /PCBM/BCP/Al	0.92	12.43	68	7.8	0.06	Non	<sup>10</sup>
ITO/NiO/CH <sub>3</sub> NH <sub>3</sub> PbI <sub>3</sub> /PCBM/Al	1.05	15.4	48	7.6	0.0725	Non	<sup>11</sup>
ITO/NiO/CH <sub>3</sub> NH <sub>3</sub> PbI <sub>3</sub> /PCBM/BCP/Al	0.901	13.16	65.38	7.75	0.06	Non	<sup>12</sup>
FTO/NiO /CH <sub>3</sub> NH <sub>3</sub> PbI <sub>3-x</sub> Cl <sub>x</sub> /PCBM/Ag	0.786	14.2	0.65	7.26	0.07	Non	<sup>13</sup>

1. J. H. Park, J. Seo, S. Park, S. S. Shin, Y. C. Kim, N. J. Jeon, H.-W. Shin, T. K. Ahn, J. H. Noh, S. C. Yoon, C. S. Hwang, S. I. Seok, *Adv. Mater.*, 2015, **27**, 4013-4019.
2. J. H. Kim, P.-W. Liang, S. T. Williams, N. Cho, C.-C. Chueh, M. S. Glaz, D. S. Ginger, A. K. Y. Jen, *Adv. Mater.*, 2014, 695-701.
3. X. Xu, Z. Liu, Z. Zuo, M. Zhang, Z. Zhao, Y. Shen, H. Zhou, Q. Chen, Y. Yang, M. Wang, *Nano Lett.*, 2015, **15**, 2402-2408.
4. W. Chen, Y. Z. Wu, J. Liu, C. J. Qin, X. D. Yang, A. Islam, Y. B. Cheng, L. Y. Han, *Energy Environ. Sci.*, 2015, **8**, 629-640.
5. K. C. Wang, P. S. Shen, M. H. Li, S. Chen, M. W. Lin, P. Chen, T. F. Guo, *ACS Appl. Mater. Interfaces*, 2014, **6**, 11851-11858.
6. Y. Bai, H. Yu, Z. L. Zhu, K. Jiang, T. Zhang, N. Zhao, S. H. Yang, H. Yan, *J. Mater. Chem. A*, 2015, **3**, 9098-9102.
7. J. Cui, F. P. Meng, H. Zhang, K. Cao, H. L. Yuan, Y. B. Cheng, F. Huang, M. K. Wang, *ACS Appl. Mater. Interfaces*, 2014, **6**, 22862-22870.
8. Z. Zhu, Y. Bai, T. Zhang, Z. Liu, X. Long, Z. Wei, Z. Wang, L. Zhang, J. Wang, F. Yan, S. Yang, *Angew. Chem. Int. Ed.*, 2014, **53**, 12571-12575.
9. K. C. Wang, J. Y. Jeng, P. S. Shen, Y. C. Chang, E. W. G. Diau, C. H. Tsai, T. Y. Chao, H. C. Hsu, P. Y. Lin, P. Chen, T. F. Guo, T. C. Wen, *Sci Rep*, 2014, **4**, 8.
10. J.-Y. Jeng, K.-C. Chen, T.-Y. Chiang, P.-Y. Lin, T.-D. Tsai, Y.-C. Chang, T.-F. Guo, P. Chen, T.-C. Wen, Y.-J. Hsu, *Adv. Mater.*, 2014, **26**, 4107-4113.
11. L. Hu, J. Peng, W. Wang, Z. Xia, J. Yuan, J. Lu, X. Huang, W. Ma, H. Song, W. Chen, Y.-B. Cheng, J. Tang, *ACS Photonics*, 2014, **1**, 547-553.
12. L. Wei-Chih, L. Kun-Wei, G. Tzung-Fang, L. Jung, *IEEE Trans. Electron Devices*, 2015, **62**, 1590-1595.
13. A. S. Subbiah, A. Halder, S. Ghosh, N. Mahuli, G. Hodes, S. K. Sarkar, *J. Phys. Chem. Lett.*, 2014, **5**, 1748-1753.

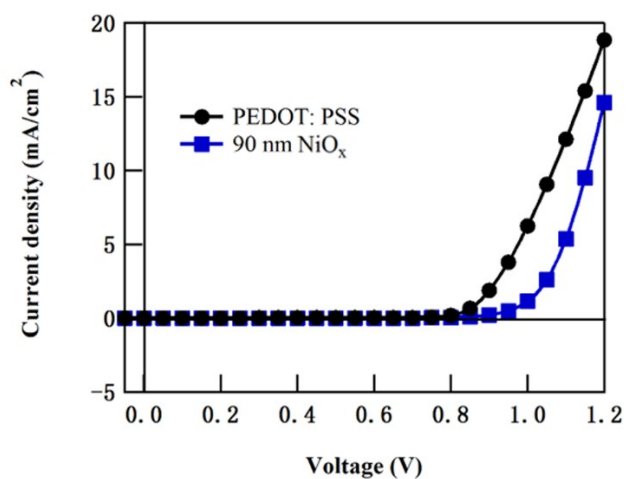


Figure S5 J-V curves for the perovskite solar cells based on the PEDOT: PSS contact and 90 nm NiO<sub>x</sub> contact.

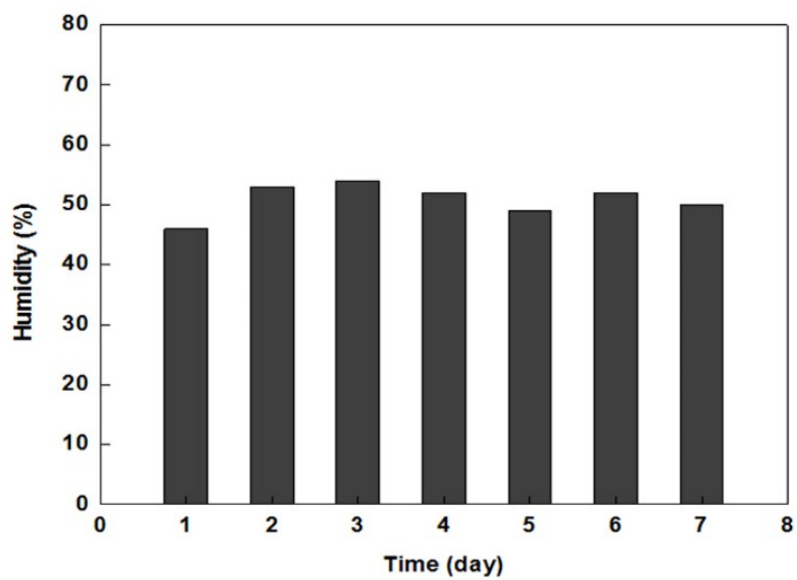


Figure S6 Ambient air humidity for the stability study.